Supplement of The Cryosphere, 15, 1187–1213, 2021
https://doi.org/10.5194/tc-15-1187-2021-supplement

The Cryosphere Open Access EGU

Supplement of

Ice content and interannual water storage changes of an active rock glacier in the dry Andes of Argentina

Christian Halla et al.

Correspondence to: Christian Halla (chris.halla@uni-bonn.de)

S1 Four phase model (4PM) sceanarios of Dos Lenguas rock glacier

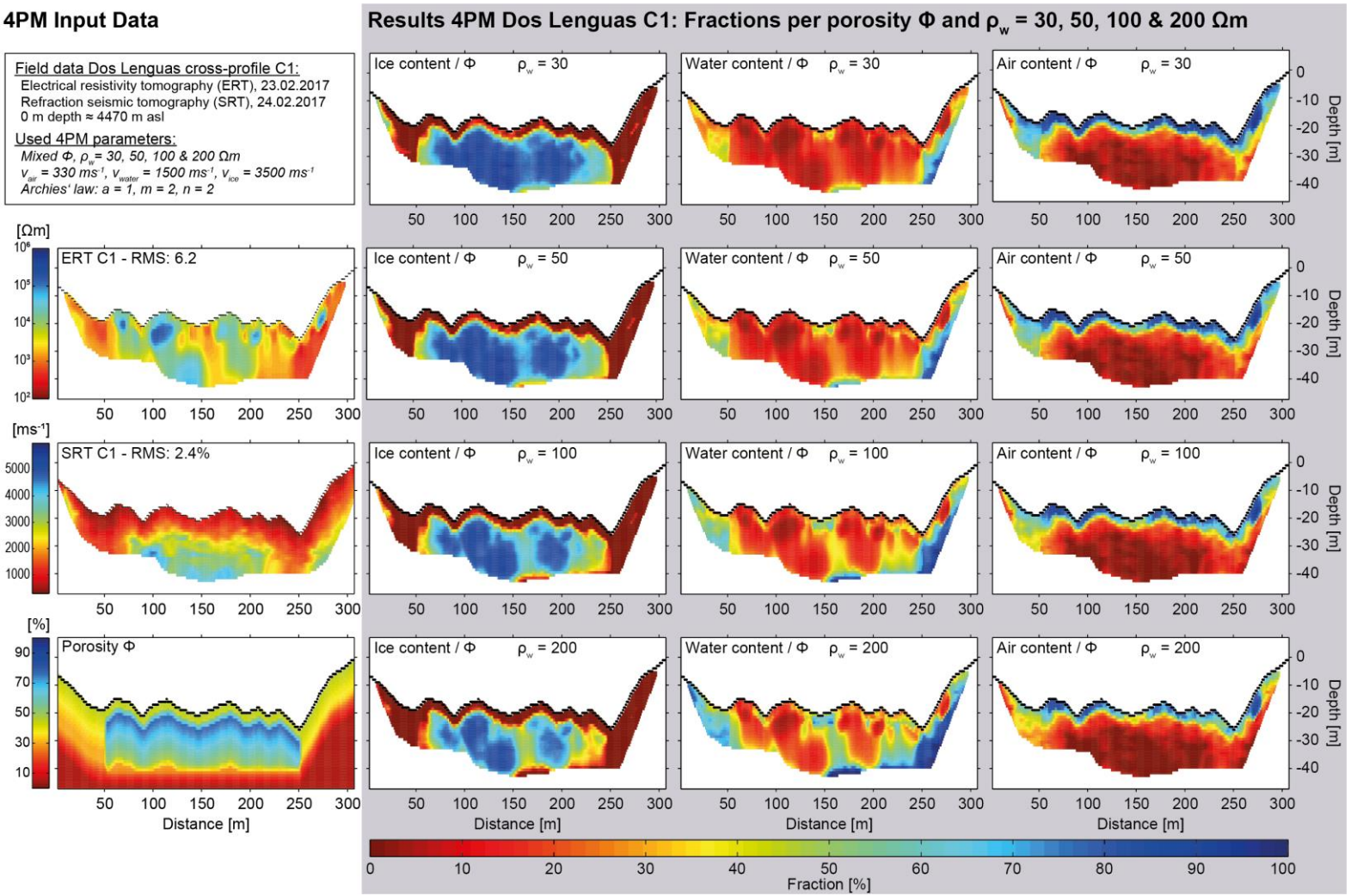

10 **Fig. S 1: 4PM results of cross-profile C1 for the mixed porosity model. Ice, water and air content per porosity (Φ) are given for four pore water resistivities (ρ_w = 30, 50, 100, 200 Ωm).**

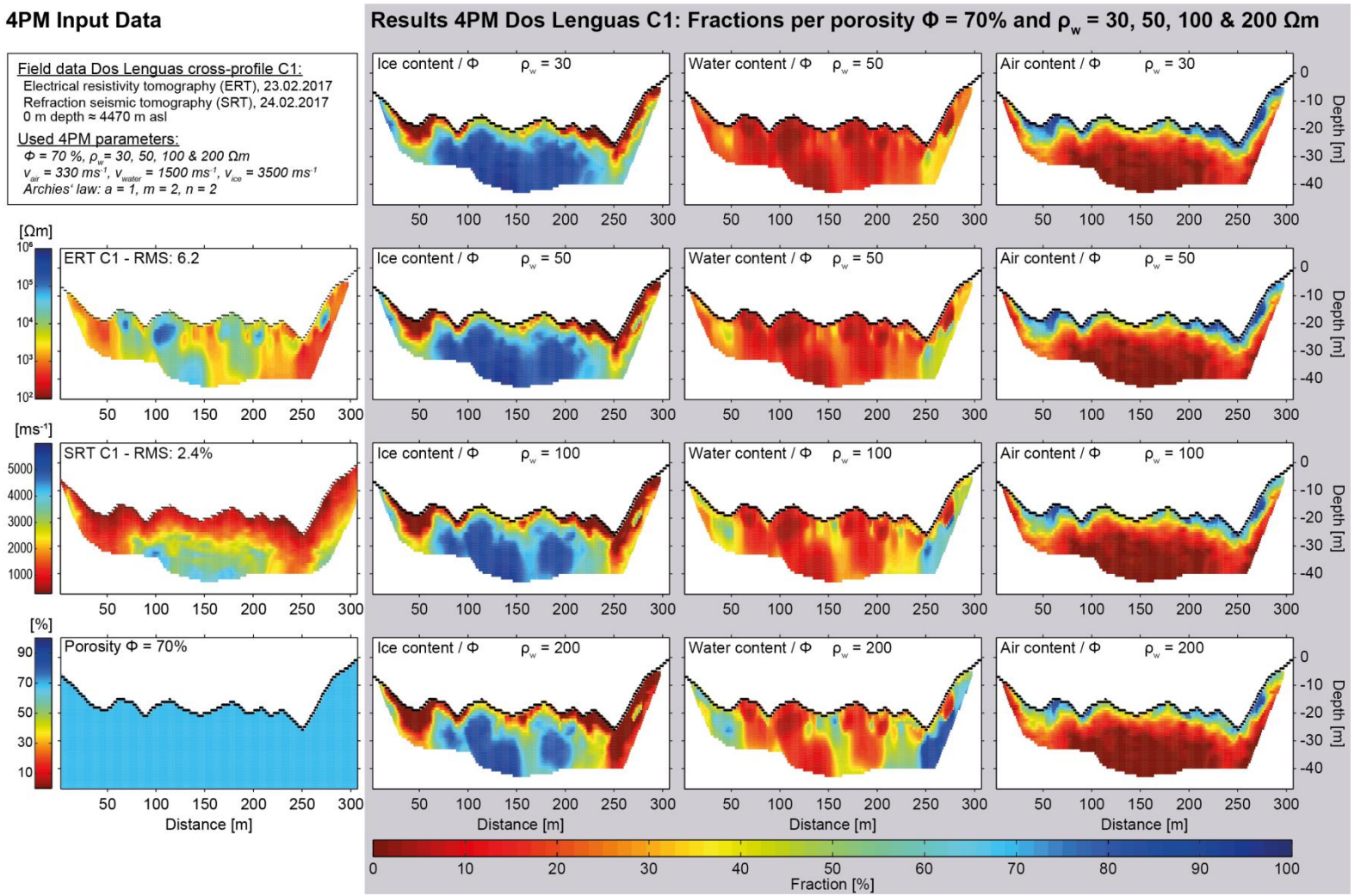

Fig. S 2: 4PM results of cross-profile C1 for the 70% porosity model. Ice, water and air content per porosity (Φ) are given for four pore water resistivities (ρ_w = 30, 50, 100, 200 Ωm).

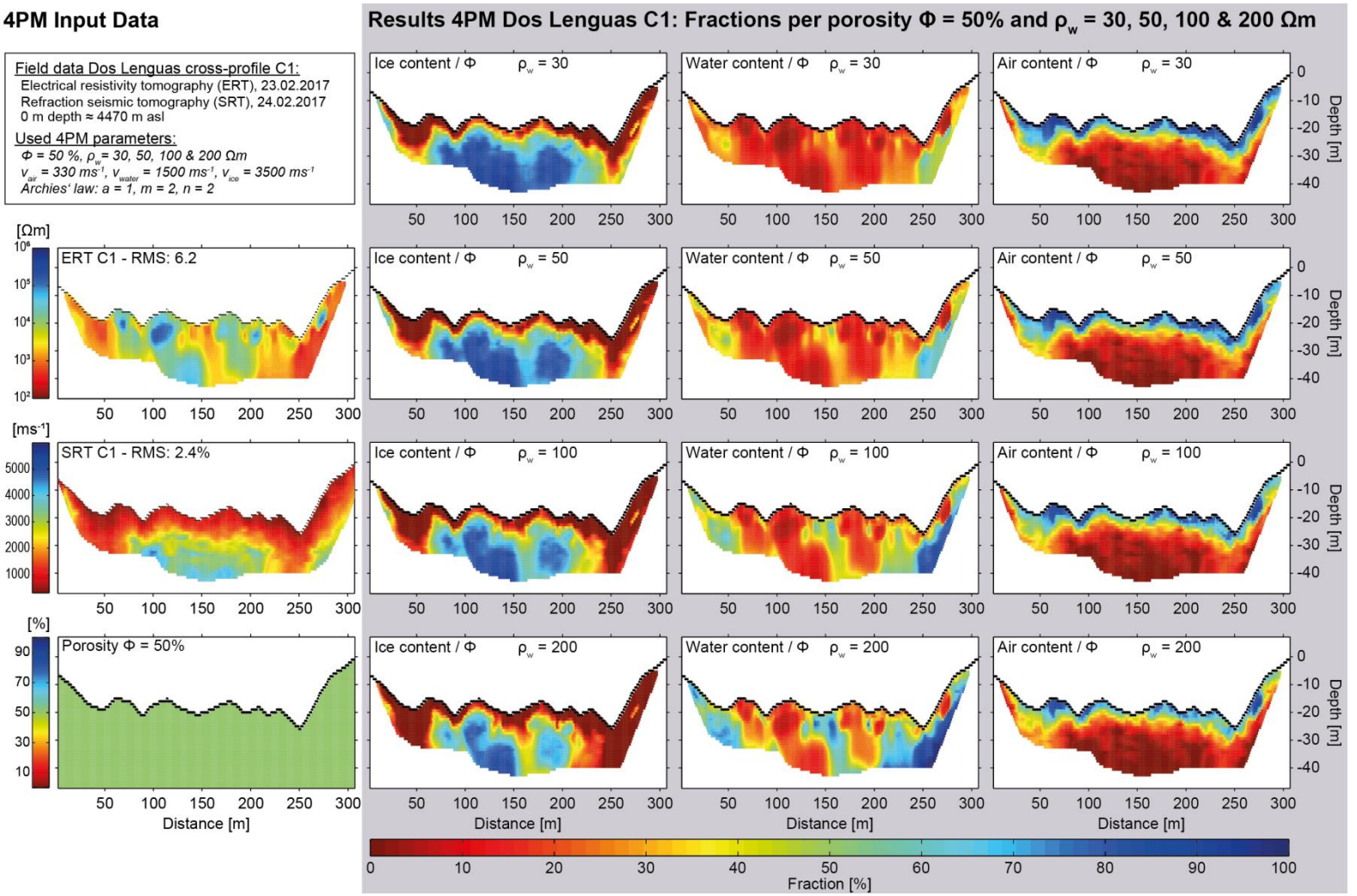

Fig. S 3: 4PM results of cross-profile C1 for the 50% porosity model. Ice, water and air content per porosity (Φ) are given for four pore water resistivities (ρ_w = 30, 50, 100, 200 Ωm).

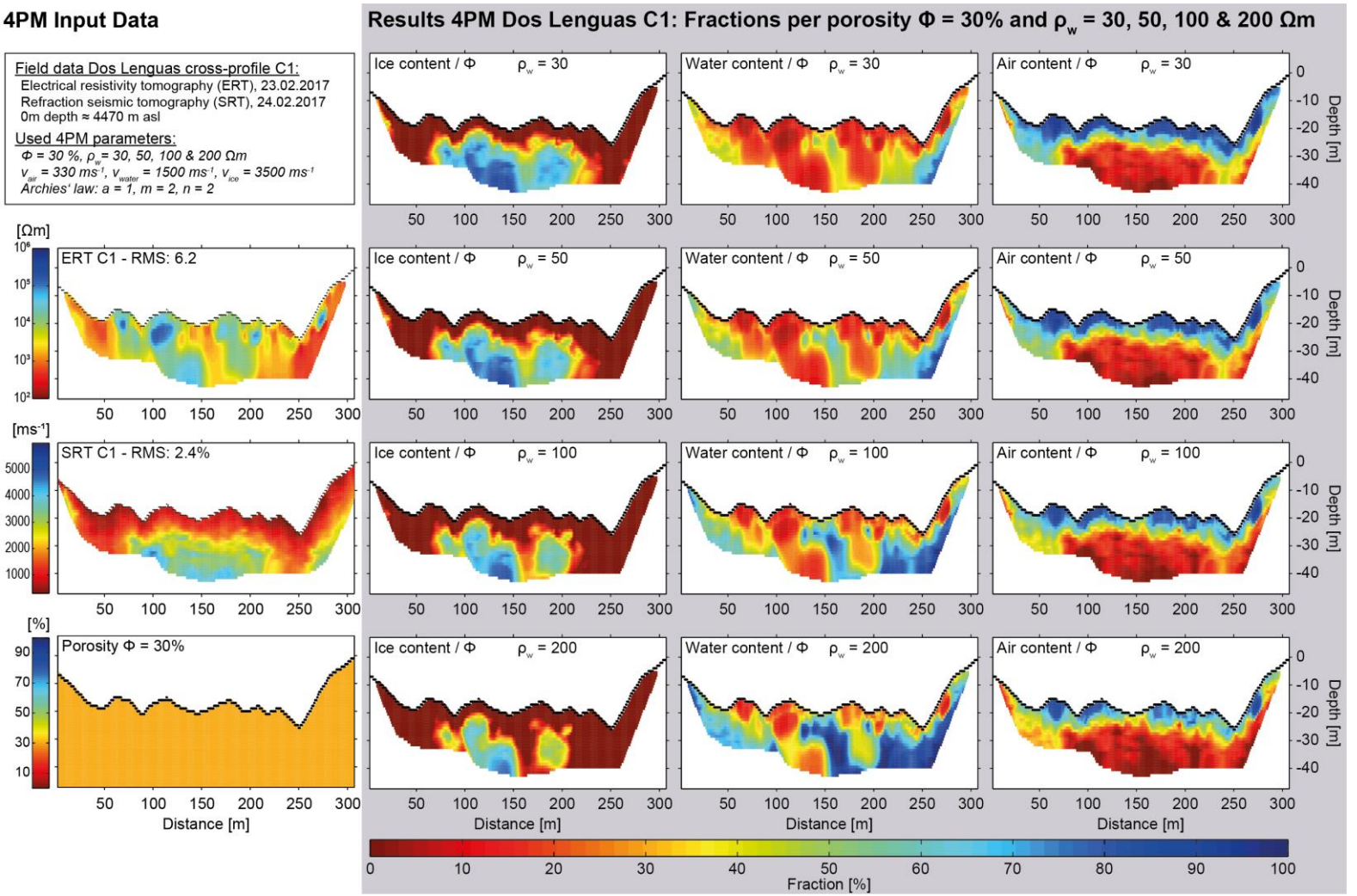

Fig. S 4: 4PM results of cross-profile C1 for the 30% porosity model. Ice, water and air content per porosity (Φ) are given for four pore water resistivities (ρ_w = 30, 50, 100, 200 Ωm).

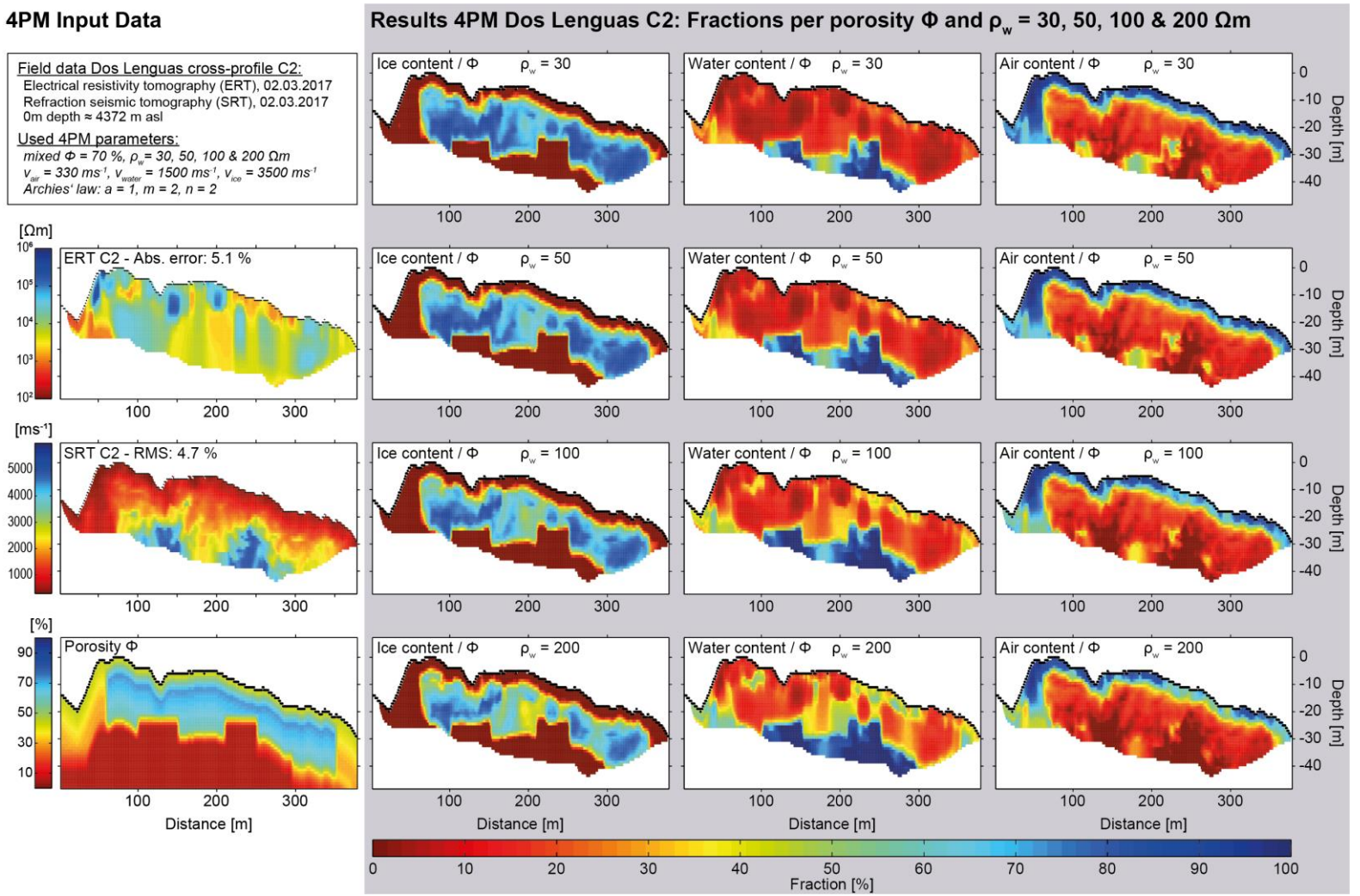

Fig. S 5: 4PM results of cross-profile C2 for the mixed porosity model. Ice, water and air content per porosity (Φ) are given for four pore water resistivities (ρ_w = 30, 50, 100, 200 Ωm).

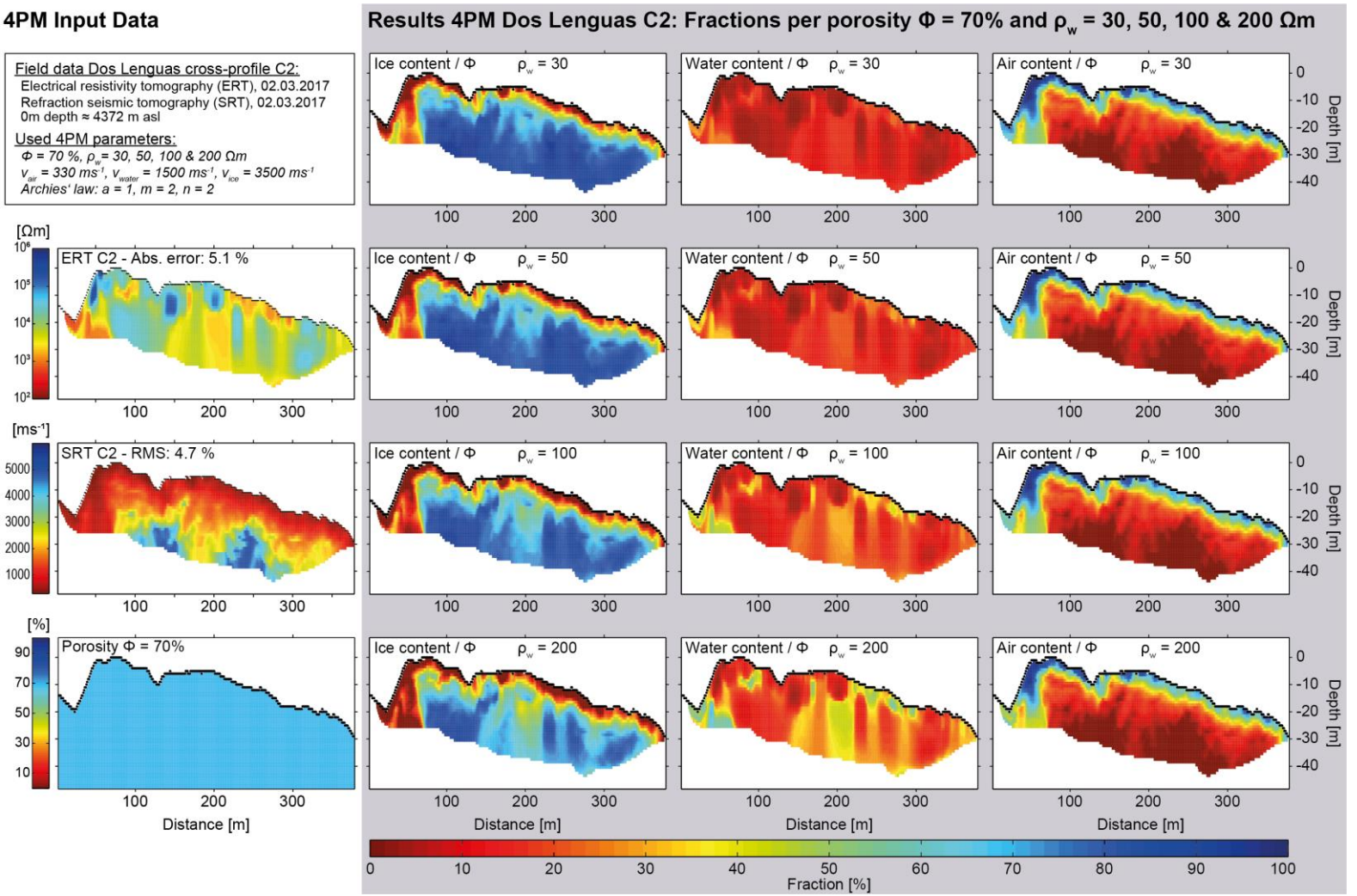

25 **Fig. S 6: 4PM results of cross-profile C2 for the 70% porosity model. Ice, water and air content per porosity (Φ) are given for four pore water resistivities (ρ_w = 30, 50, 100, 200 Ωm).**

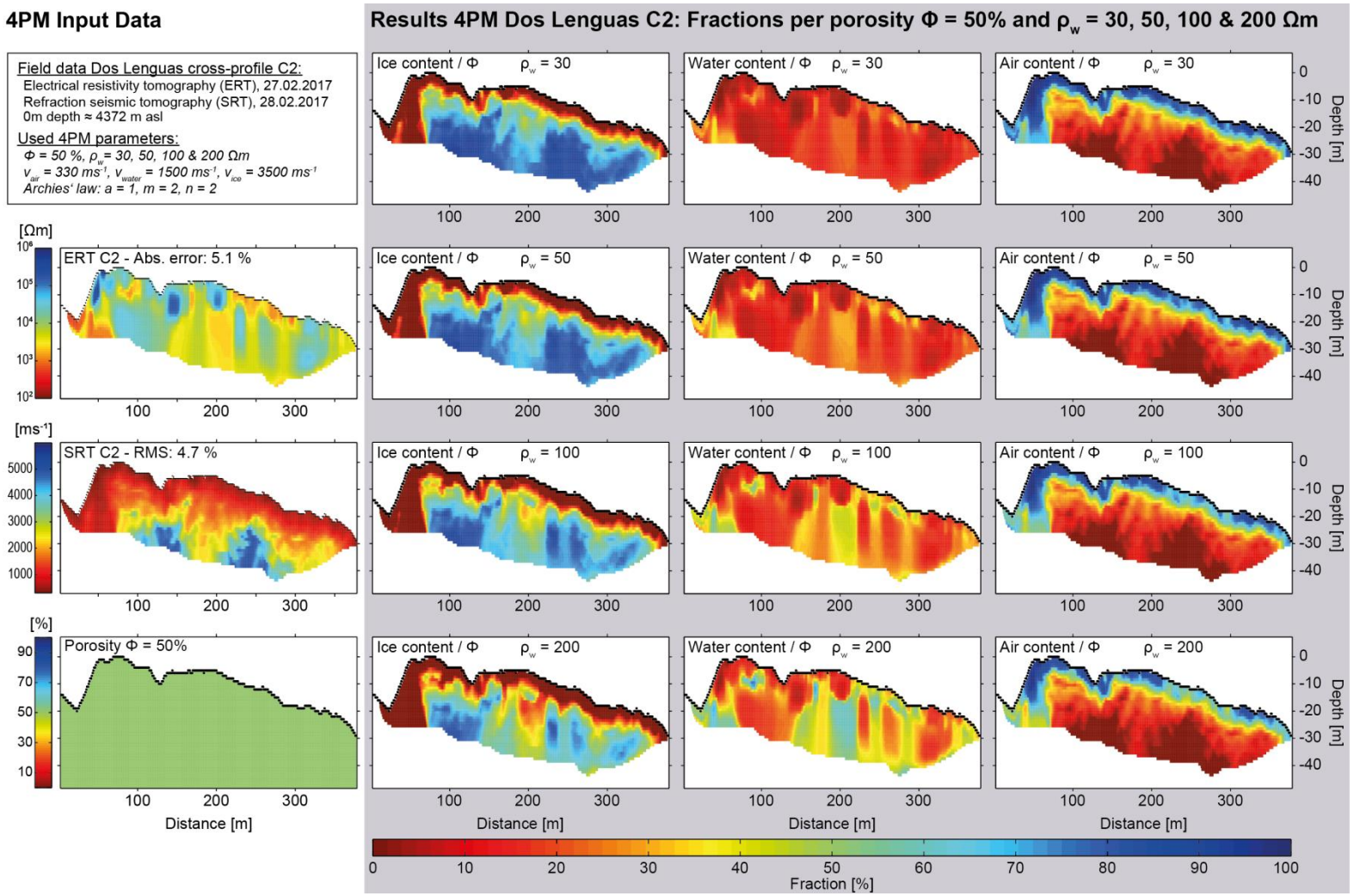

Fig. S 7: 4PM results of cross-profile C2 for the 50% porosity model. Ice, water and air content per porosity (Φ) are given for four pore water resistivities (ρ_w = 30, 50, 100, 200 Ωm).

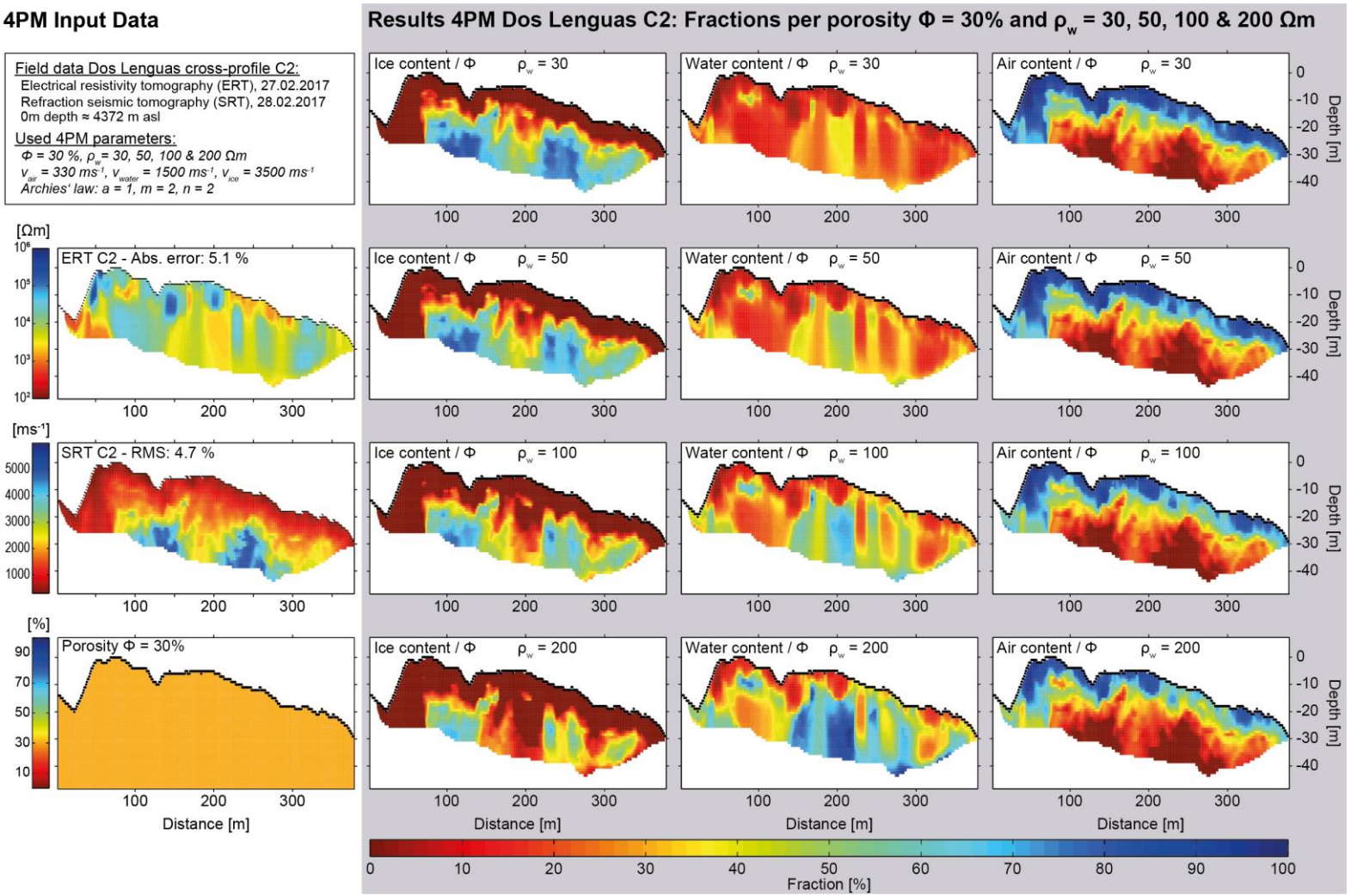

Fig. S 8: 4PM results of cross-profile C2 for the 30% porosity model. Ice, water and air content per porosity (Φ) are given for four pore water resistivities (ρ_w = 30, 50, 100, 200 Ωm).

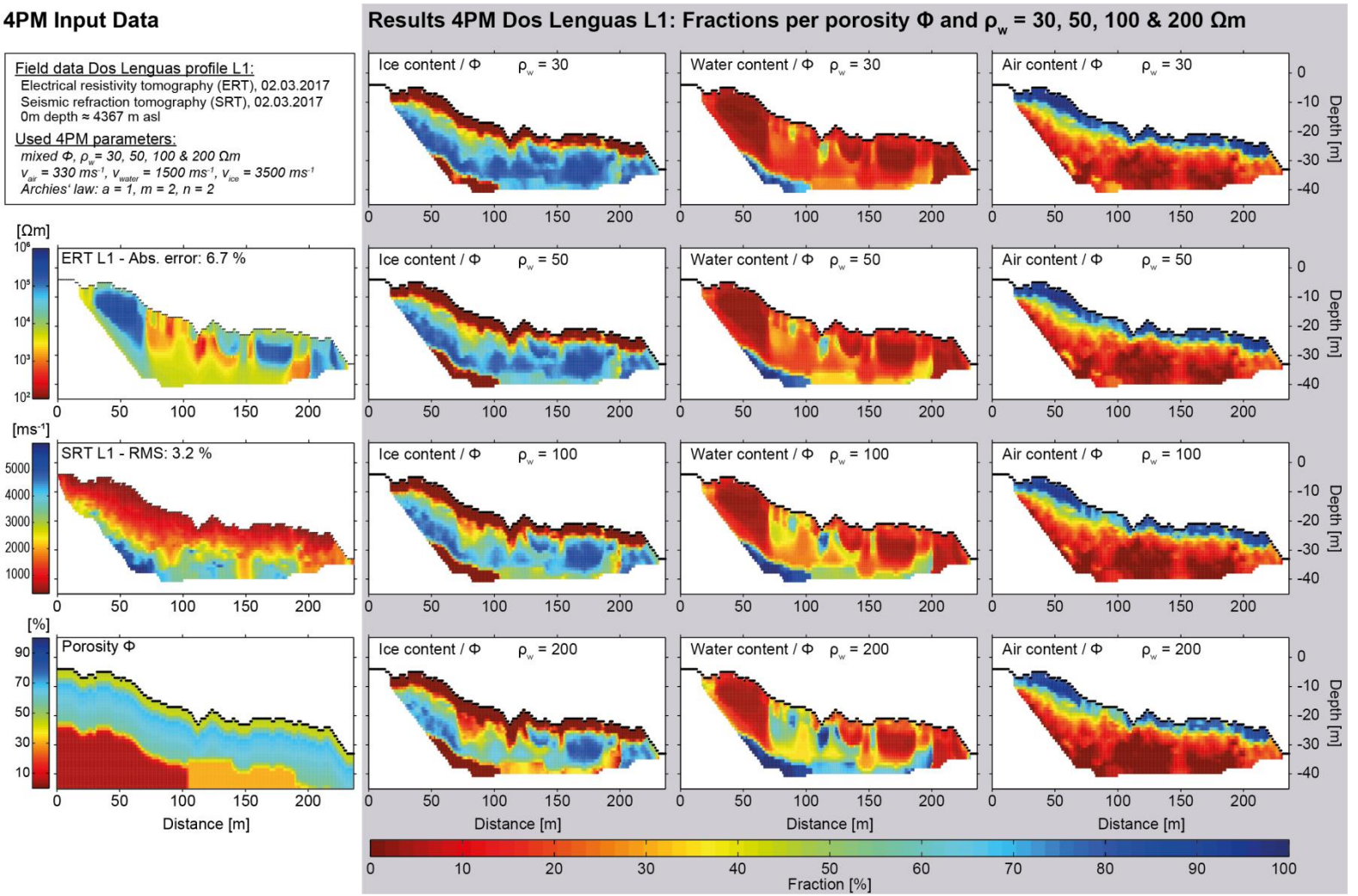

Fig. S 9: 4PM results of cross-profile L1 for the mixed porosity model. Ice, water and air content per porosity (Φ) are given for four pore water resistivities (ρ_w = 30, 50, 100, 200 Ωm).

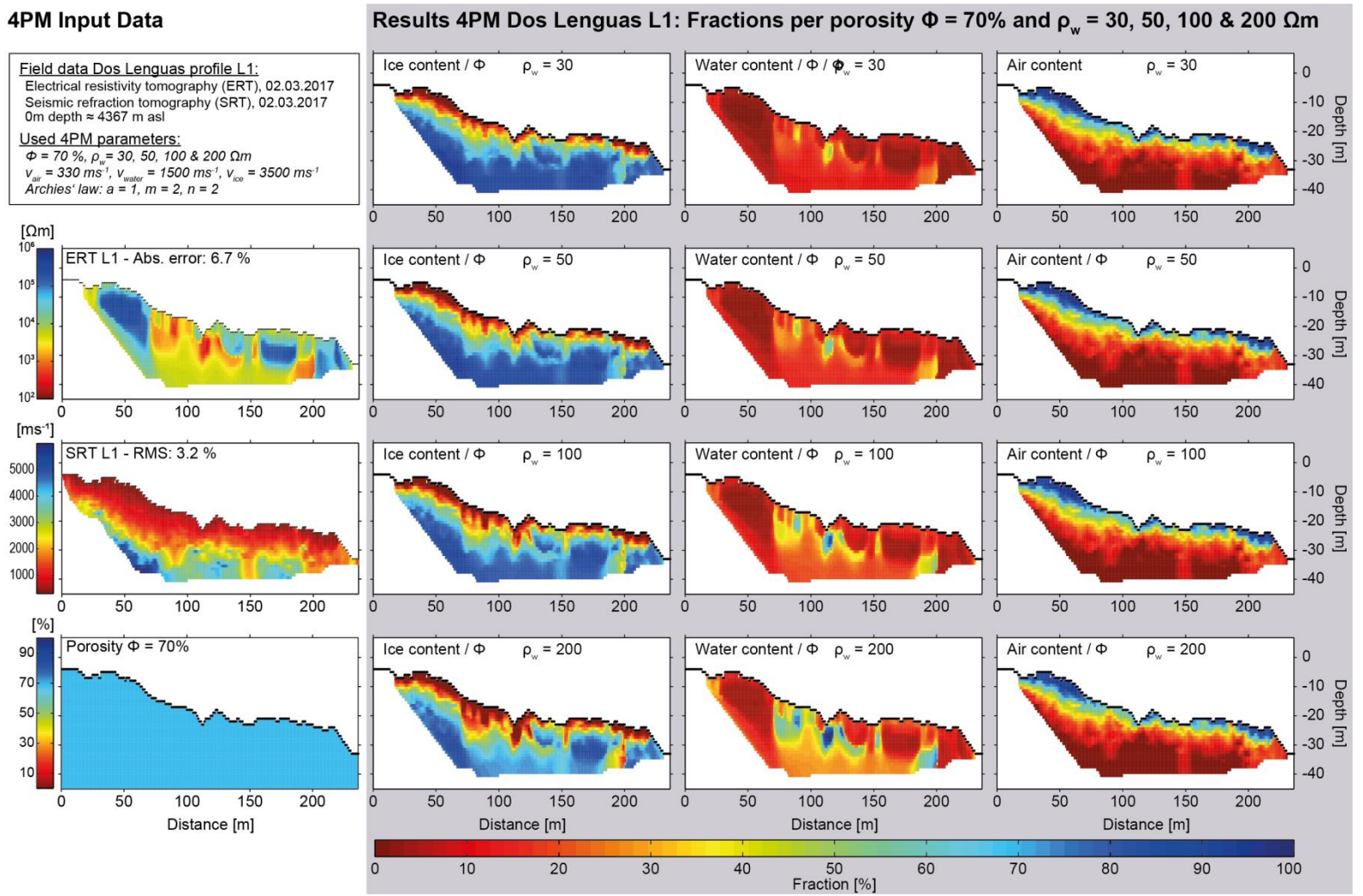

Fig. S 10: 4PM results of cross-profile L1 for the 70% porosity model. Ice, water and air content per porosity (Φ) are given for four pore water resistivities (ρ_w = 30, 50, 100, 200 Ωm).

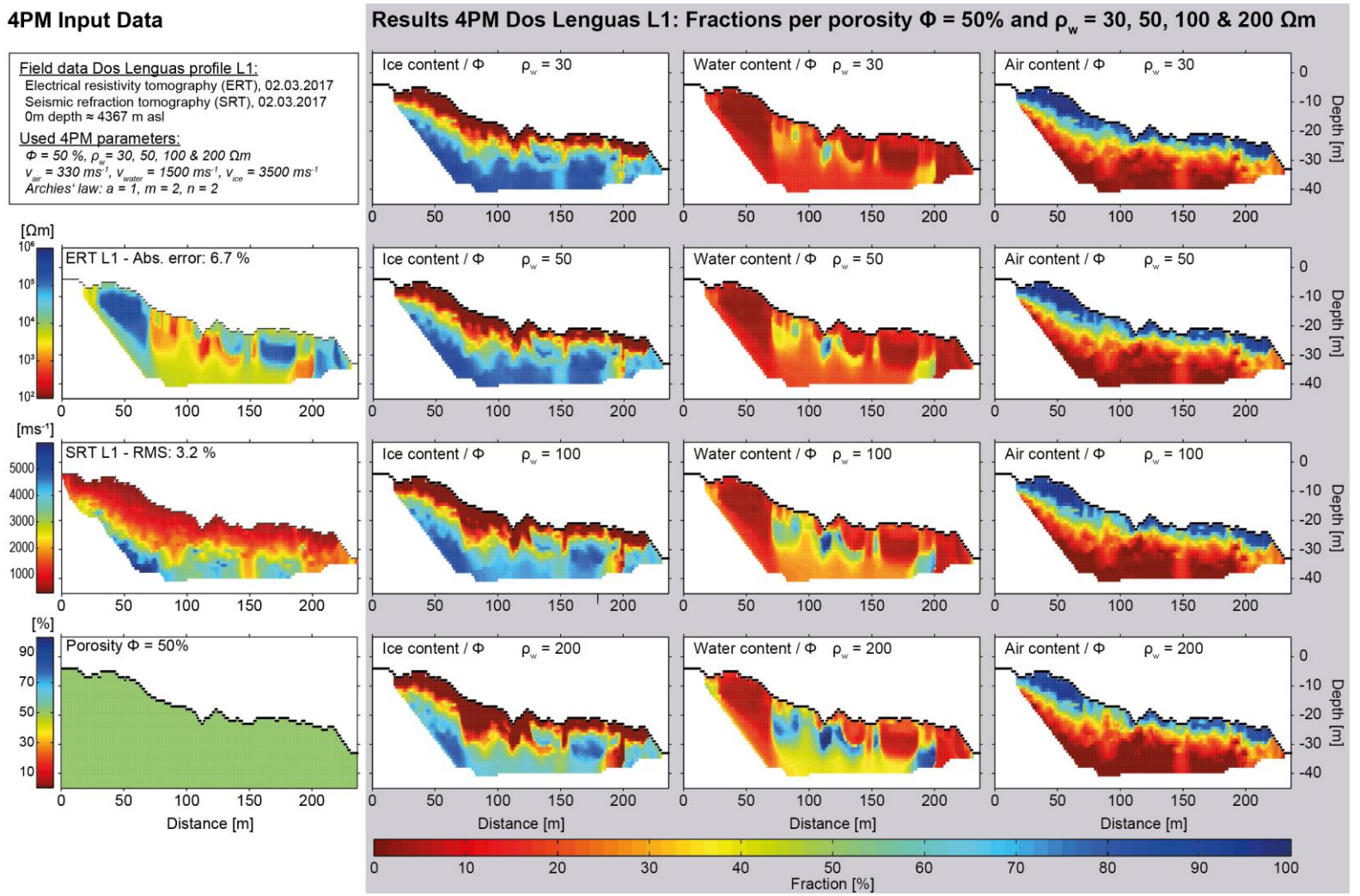

40 **Fig. S 11: 4PM results of cross-profile L1 for the 50% porosity model. Ice, water and air content per porosity (Φ) are given for four pore water resistivities (ρ_w = 30, 50, 100, 200 Ωm).**

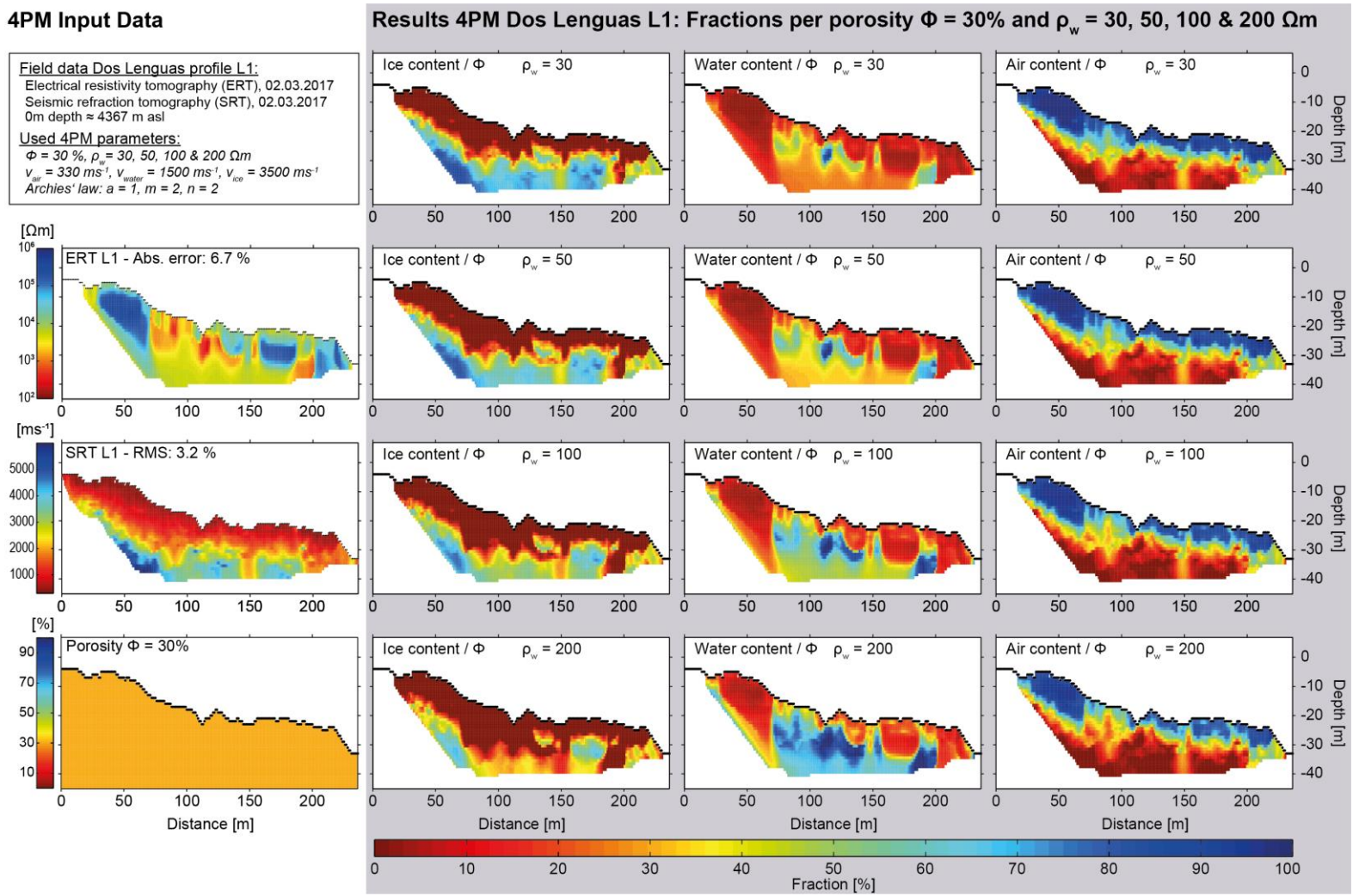

Fig. S 12: 4PM results of cross-profile L1 for the 30% porosity model. Ice, water and air content per porosity (Φ) are given for four pore water resistivities (ρ_w = 30, 50, 100, 200 Ωm).

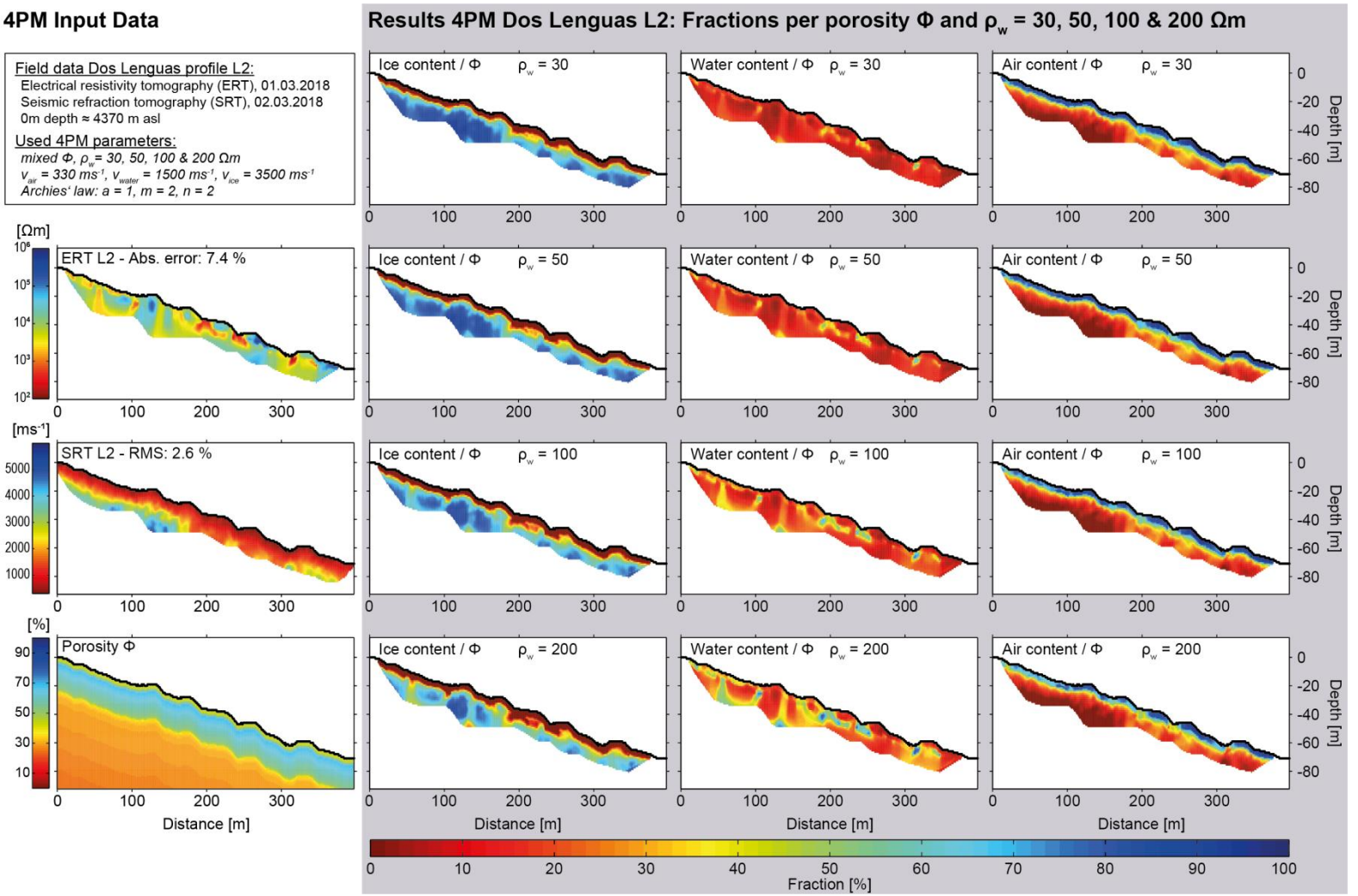

Fig. S 13: 4PM results of cross-profile L2 for the mixed porosity model. Ice, water and air content per porosity (Φ) are given for four pore water resistivities (ρ_w = 30, 50, 100, 200 Ωm).

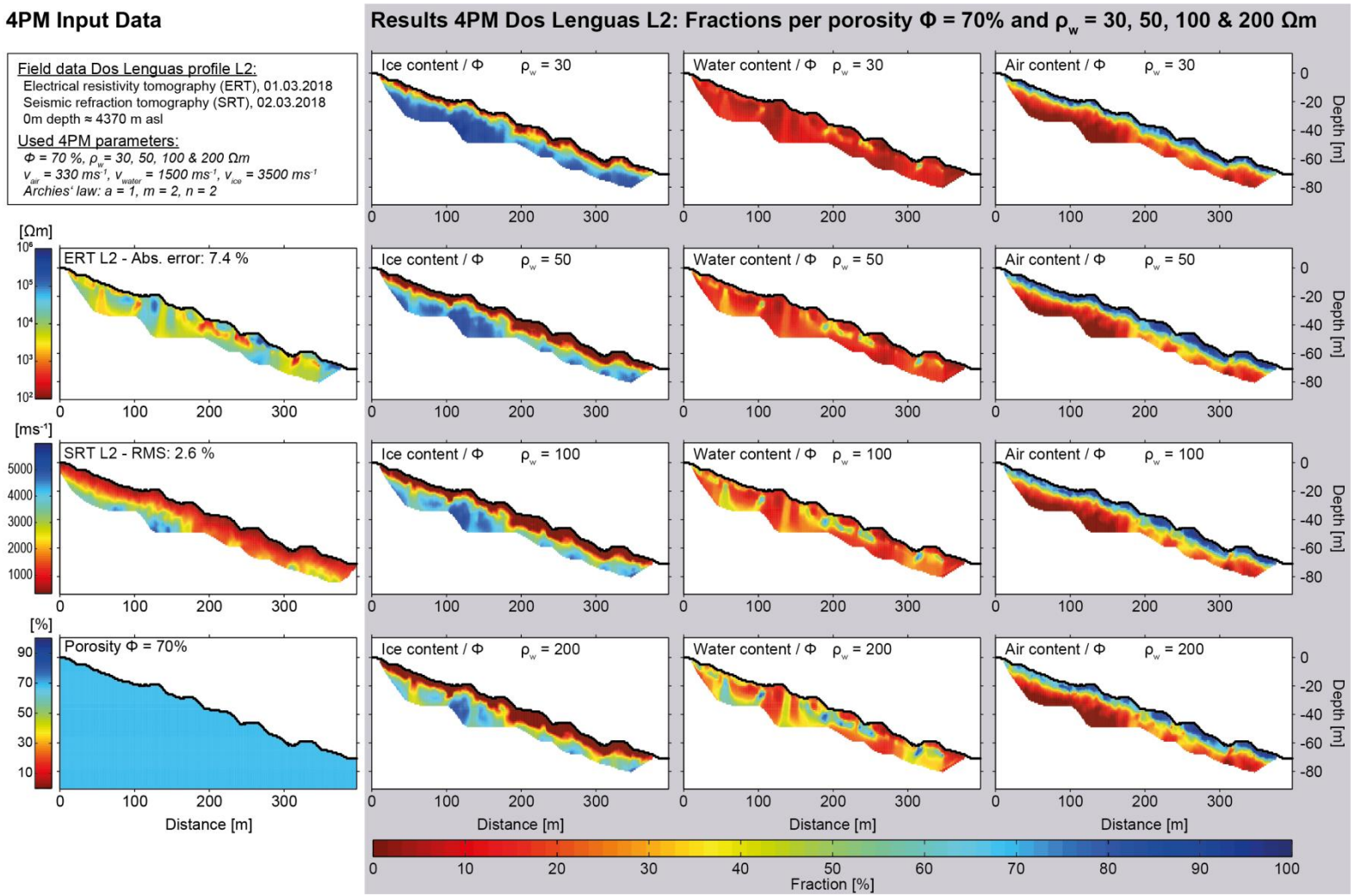

Fig. S 14: 4PM results of cross-profile L2 for the 70% porosity model. Ice, water and air content per porosity (Φ) are given for four pore water resistivities (ρ_w = 30, 50, 100, 200 Ωm).

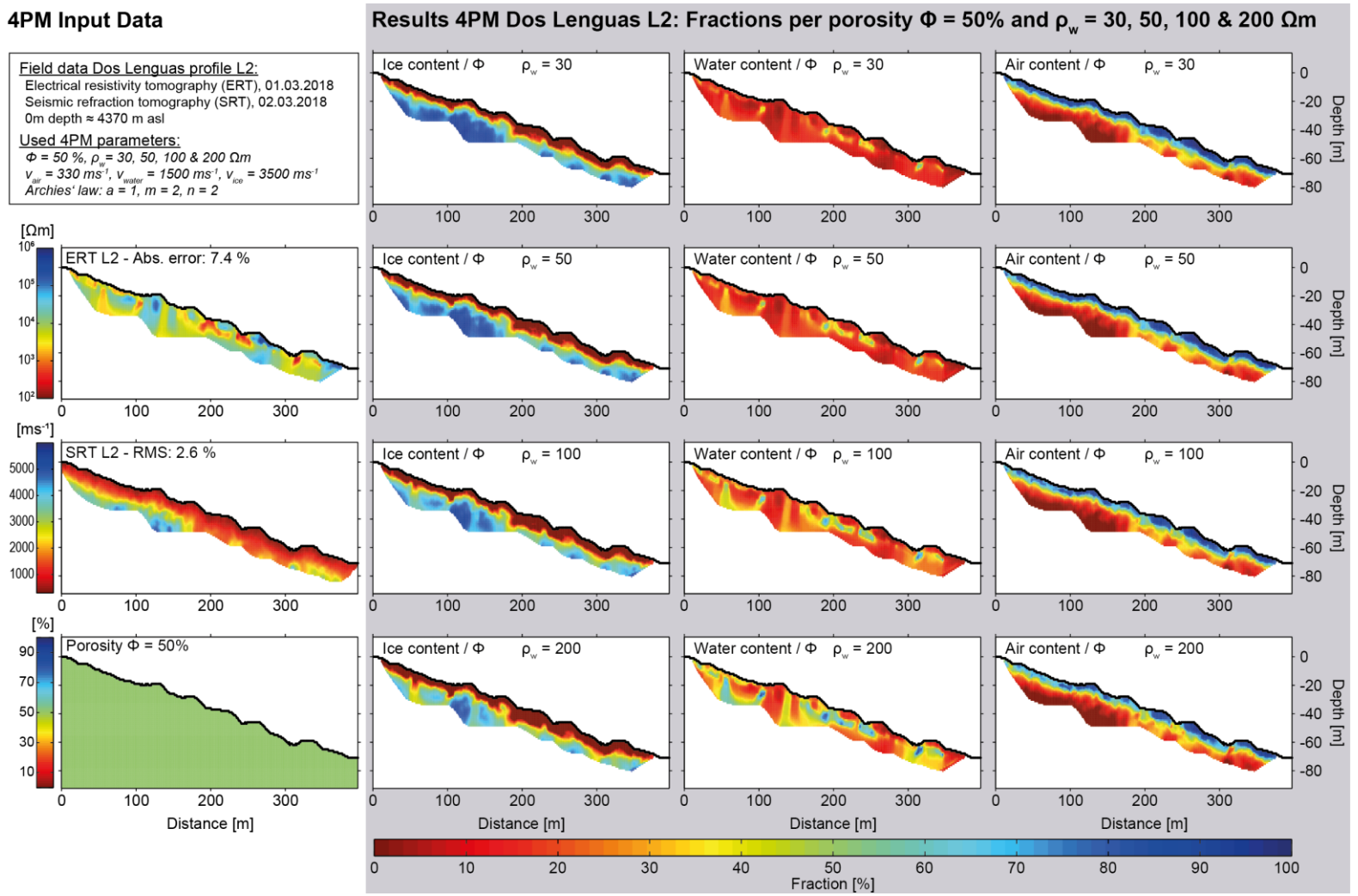

Fig. S 15: 4PM results of cross-profile L2 for the 50% porosity model. Ice, water and air content per porosity (Φ) are given for four pore water resistivities (ρ_w = 30, 50, 100, 200 Ωm).

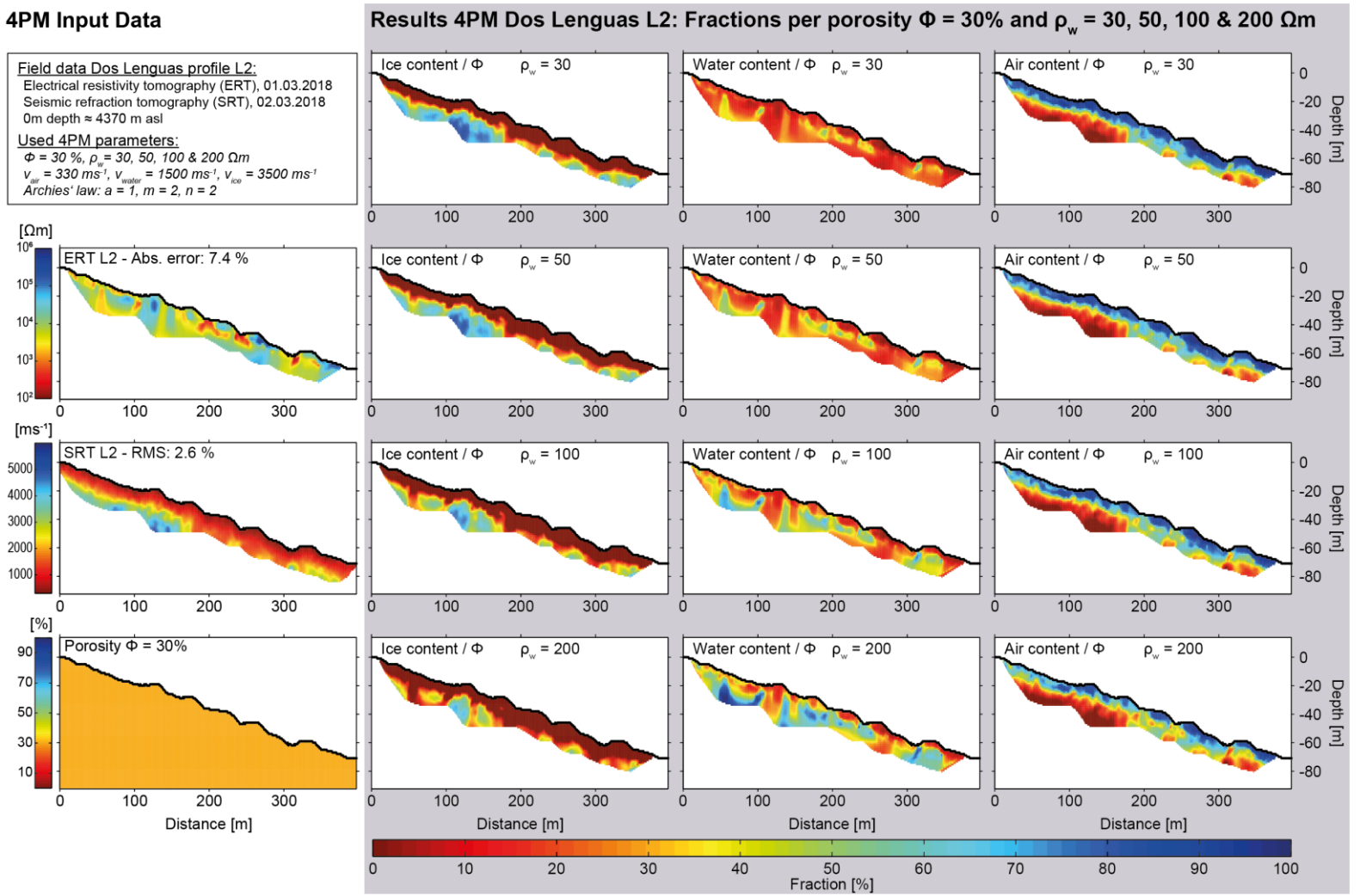

55 **Fig. S 16: 4PM results of cross-profile L2 for the 30% porosity model. Ice, water and air content per porosity (Φ) are given for four pore water resistivities (ρ_w = 30, 50, 100, 200 Ωm).**

S2 Ground surface temperatures of Dos Lenguas rock glacier

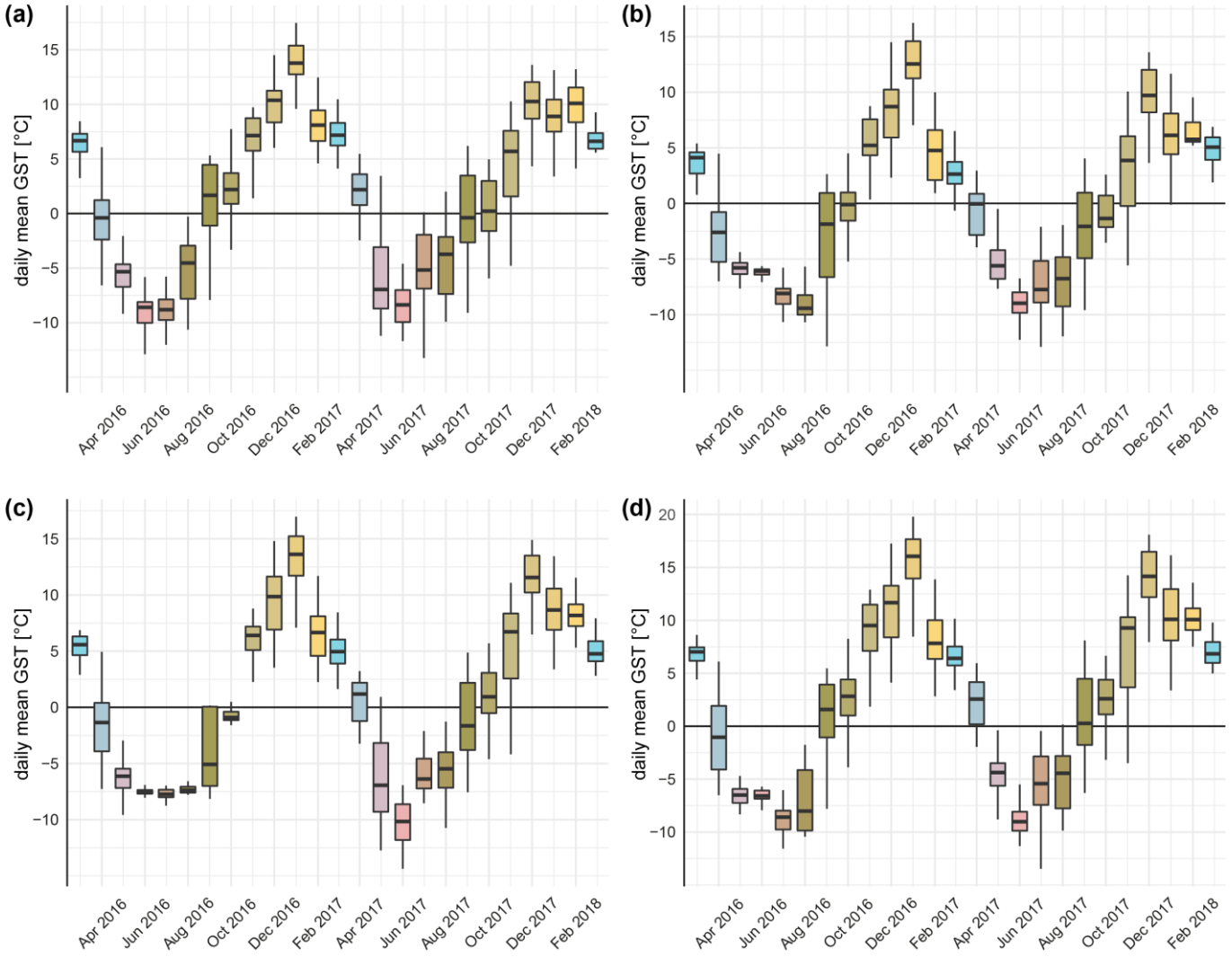

Fig. S 17: Boxplots of daily mean ground surface temperatures (GST) from Mar 2016 to Mar 2018 measured with iButtons in three hour intervals at four different locations of Dos Lenguas rock glacier ((a), (b), (c), and (d)). The ground surface temperature regime during the ablation period between Sep 2016 and Mar 2017 shows an earlier and warmer spring (Sep 2016) and a later and higher temperature maximum during summer (Jan 2107) compared to the ablation period 2017-18.